

Augmentation of Heat Transfer Characteristics for Flow Through Circular Tube by Radial Guide Vane Swirl Generators

تحسين خصائص انتقال الحرارة للسريان خلال أنبوبة دائرية باستخدام ريشة توجيه ملتوية.

G. I. Sultan

Assoc. Prof., Mechanical Power Dept.,
Faculty of Engineering, Mansoura University, Egypt.
Email: gisultan@mans.edu.eg

الخلاصة:

تم تحسين معامل انتقال الحرارة بالحمل من أنبوبة ذات فيض حراري منتظم باستخدام ريشة توجيه ملتوية. تم دراسة تأثير إضافة ريش التوجيه الملتوية على معامل انتقال الحرارة عمليا. وأثناء إجراء التجارب تم تغيير رقم رينولدز من 2747 إلى 6390 ومكان الريشة الملتوية تأثير ليكون $x/L = 0, 0.25, 0.5, 0.75, 1.0$. وقد بينت النتائج أن استخدام ريشة توجيه ملتوية أدى إلى تحسين معامل انتقال الحرارة عن الأنبوبة الملساء وأن وضع الريشة الملتوية عند $S_1/L = 0.25$ من دخول الأنبوبة أعطت أفضل تحسين لخصائص انتقال الحرارة. وقد تم صياغة النتائج المعملية في علاقة لا بعدية لتعطي رقم نوسلت كدالة في رقم رينولدز وموضع الريشة الملتوية اللا بعدى. كما بينت النتائج أيضا أن أكبر تحسن في كفاءة انتقال الحرارة تم الحصول عليه هو 277%.

Abstract:

The convective heat transfer coefficient for a uniform heat flux tube is improved experimentally by using a single twisted vanes turbulator. The effect of the twisted vane inserts on the heat transfer rate are studied experimentally. During this study, the operating parameters are Reynolds number (2747-6390), and local position of the swirl element ($S_1/L=0.0, 0.25, 0.5, 0.75, 1.0$). The results demonstrated that the use of twisted vane swirl element inserts leads to a higher heat transfer coefficient rather than that of plain tube and the swirl element position of 0.25 from tested tube inlet yields a better heat transfer characteristics. The results are also correlated in the form of Nusselt number as a function of Reynolds number and turbulator position ratio. An augmentation of heat transfer coefficient up to 277% is obtained.

Keywords: Heat transfer enhancement; friction factor; swirl flow, and forced convection.

1. Introduction:

In the past decade, heat transfer enhancement technology has been developed and widely applied to the heat exchanger applications. For example, refrigeration, automotives, industrial process, solar water heating,....., etc. There has been a great attempt to reduce the size and cost of the heat exchanger, and energy consumption. The most significant variable in reducing the size and cost of the heat exchanger is the heat transfer coefficient and pressure drop which generally leads to less capital cost. In general, enhancing heat transfer can be classified into two groups. One is the passive method, such as a surface coating, rough surfaces, extended surfaces, swirl flow devices, the twisted tubes, twisted tap inserts, and additives for liquid and gases. The other is the active method, which requires extra external power sources, for

example, mechanical aids, surface vibration, injection and suction of fluid from the boundary layers, jet impingement and use of electrostatic fluid. The swirl flow devices can be classified into two kinds: the first is the continuous swirl flow and the other is the decaying swirl flow. The use of decaying swirl flow is one of the promising techniques for augmentation of convective heat transfer. Many researches has been directed to study the different mechanisms for heat transfer enhancement. A lot of studies on full-length twisted tape [2-6] have been carried out, and it is found that the use of twisted tapes improve the thermal performance associated with increasing the pressure drop. Leonard et. al [7], investigated experimentally the effect of internal fins with a star-shape cross-section on heat transfer and pressure drop in a counter flow heat exchanger using air as a working fluid. They found that heat transfer

is increased by about 12-51 % over plain tube value. Watcharin et al. [8], investigated experimentally the influence of twisted tape inserts on heat transfer, Nusselt number, and friction factor in a double pipe heat exchanger. They found that the maximum Nusselt number for using these enhancement devices is 188% higher than that of plain tube. Noothong et al., [9] studied the effect of V-shape nozzle turbulators on the heat transfer and friction factor in a circular tube. They found that the nozzle turbulators have a significant effect on the heat transfer. Promvong and Eiamsa-ard[10], investigated experimentally the heat transfer, and friction factor in a circular tube at constant heat flux filled with conical rings turbulators and a twisted tape swirl generator. They found that the average heat transfer rates when using both the conical rings and twisted tape of different twist ratio of 3.75 to 7.5 are found to be 367% and 350%, respectively over the plain tube. Paisarn [11], presented the heat transfer characteristics and pressure drop in the corrugated channel under constant heat flux. He found that the average Nusselt number increased with both Reynolds number, heat flux and wavy angle. Mehmet et al. [12], studied the effect of geometry of the deflecting element in the radial guide vane swirl generator on the heat transfer and fluid friction in decaying swirl flow which has three different configurations: swirl generator with conical deflecting element, with spherical deflecting element and with no deflecting element. They found that the average Nusselt number is increased up to 99% , 119%, and 148%, for the first, second and third type swirl generator, respectively. Smith et al. [13], reported through an experimental work the pressure drop and heat transfer characteristics of flow through circular tube with twisted tape inserts at free spacing of $s=2p$, $3p$, and $4p$, respectively and Reynolds number varied from 2300 to 7500.

They concluded that the free spacing twisted tapes with $s=2p$ gave a heat transfer lower

than full length twisted tape around 5-15% while it can be decreases the pressure drop around 90%. Ebru et al. [14] studied experimentally the effect of swirl motion on the hot air by placing swirl elements of various diameters and the number of circular holes in straight or zigzag line rows on the entrance region of an inner pipe of a concentric heat exchanger. They found that the heat transfer rate increases with decreasing diameter and number of holes of the swirl element and the maximum enhancement was about 130% in a counter current flow with swirl element having smaller diameter five holes in a narrow zigzag line. Hong et al.[15] studied the heat transfer of a converging-diverging tube with evenly spaced twisted-tapes and found that the twisted-tape with twist ratio of 4.72 and the rotation angle 180° has the best performance. Smith et al. [16], investigated experimentally the heat transfer and friction factor employing louvered strips inserted in a concentric tube. Their results confirmed that the increase in average Nusselt number and friction loss for the inclined forward louvered strip were 284% and 413% while those for the backward louvered strip were 263% and 233% over the plain tube, respectively.

From the previous review, a lot of researchers have been used a twisted tape, rough surfaces, different guide vanes swirl generators and injection secondary stream into the boundary layer to enhance the heat transfer coefficient. So, the present work is concerned through an experimental study to detect the local position of a decaying guide vane swirl generator inside the tube.

2. Experimental Apparatus:

The arrangement of the experimental apparatus and details of the test section are shown in figures 1 and 2. The tested tube (1) is made from brass, 45 cm long, 34 mm inside diameter, and 2 mm thickness.

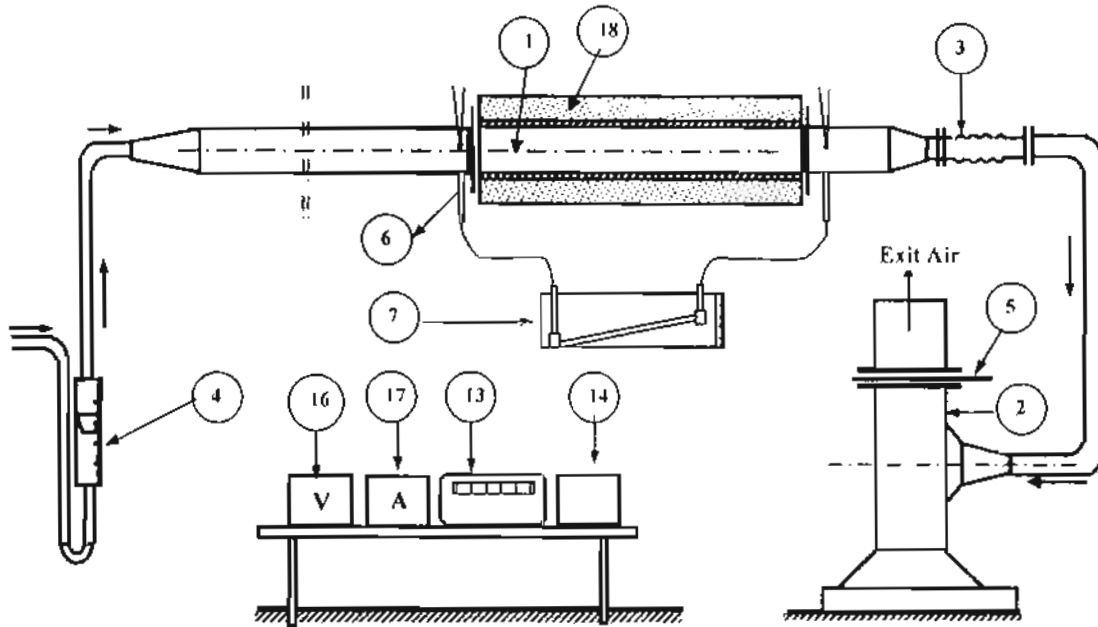


Fig. 1 The experimental test rig and measuring devices.

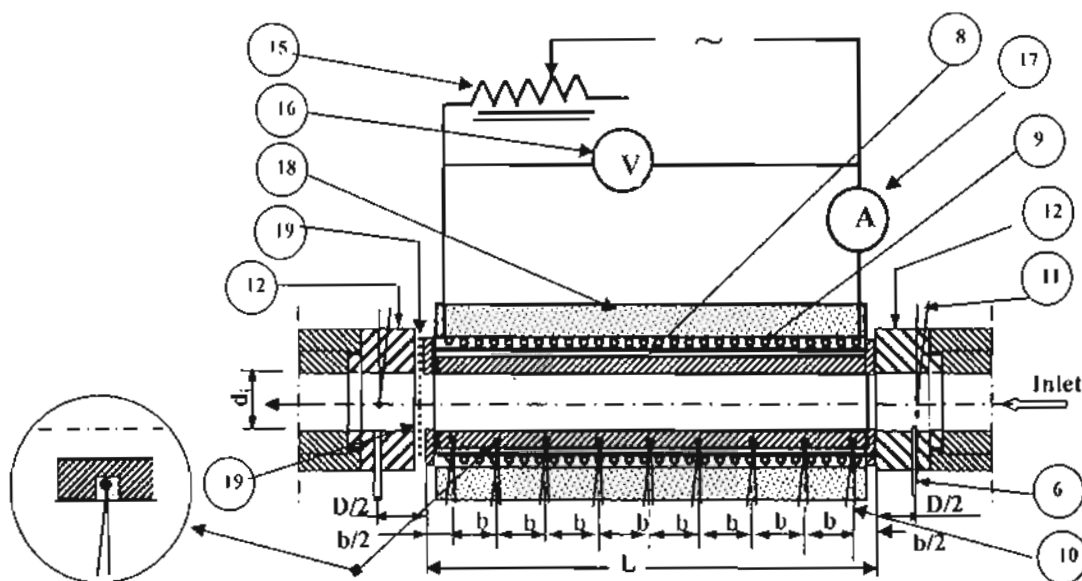


Fig.2 Detailed of the test

- | | | | | |
|---------------------|---------------------------|---------------------------------------|----------------------|-------------------------|
| 1. Tested tube. | 2. Air blower. | 3. Flexible connection. | 4. Rotameter. | 5. Plate gate. |
| 6. Pressure tapes. | 7. Inclined manometer. | 8. Mica-sheet. | 9. Electric heater. | 10., 11. Thermocouples, |
| 12. Teflon junction | 13. Temperature recorder, | 14. Multi-switch point selector | 15. Auto-transformer | 16. Voltmeter |
| 17. Ammeter | 18. Thermal insulation | 19. Radial guide vane swirl generator | | |

$$L = 45 \text{ cm} \ \& \ d_i = 34 \text{ mm} \ \& \ d_o = 38 \text{ mm}$$

The 2.5 kW air blower (2) is used to withdraw air to the test section through a flexible connection (3). The air flow rate which is passing through the test section is measured by a rotameter (4) and adjusted by control gate plate (5). Two pressure taps (6)

are located in the vicinity of the test section, 10 mm from inlet and outlet of the test section. The pressure drop across the test section is measured by an inclined U-tube water manometer (7). The outside surface of the test section is electrically insulated with

1 mm mica sheet (8), and is wrapped with the electric resistance (9) (1 mm wire diameter, 8 Ω electric resistance). The hydrodynamic entry section is long enough to accomplish fully developed flow at inlet to the test section. The outside wall temperature of the tested tube is measured by nine copper-constantan thermocouples (10), 50 mm apart. To reduce the back conduction of heat from the heated to the unheated sections in the longitudinal direction, two Teflon connections (12), are fixed at both inlet and outlet of the test section. Two thermocouples (11) are fixed at inlet and at the outlet of the test section at the midplane to measure the air temperature. All thermocouples are connected to a temperature recorder (13) which has an accuracy of $\pm 0.1^\circ\text{C}$ through a multi-switch points selector (14). All thermocouples are calibrated and the accuracy is found to be within $\pm 0.1^\circ\text{C}$. AC power supply is provided to the heating coil (9) and controlled by an auto-transformer (15). The volt and electric current through the heating coil is measured by voltmeter (16) and ammeter (17), respectively as shown in Fig.(2). The tested tube is covered with 50 mm glass wool insulation, (18) to decrease the heat loss to a negligible value. The twisted guide vane swirl generator (19) which is shown in Fig. 3, is made from copper and fixed by interference at the specified position, ($S/L=0.0, 0.25, 0.5,$ and 1.0 from test section inlet).

For each run, it is necessary to record the data of temperature, air volume flow rate, and pressure drop at steady state conditions. The experimental error estimation is made based on the accuracies of instruments which measure the individual quantities. The steady state condition of flow is reached after about 90 minutes depending on the flow velocity.

The accuracies of the thermocouples and rotameter are within $\pm 1^\circ\text{C}$ and $\pm 0.2\%$ of the full scale, respectively. The uncertainties in calculating Reynolds number, Nusselt number, and pressure drop are calculated to be $\pm 5.2\%$, $\pm 8.4\%$, and $\pm 6\%$, respectively.

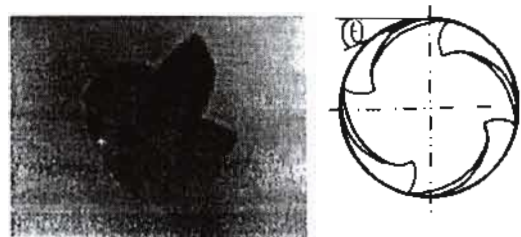


Fig. (3) The Photo-graph and line drawing of the twisted vane turbulator element

3. Data Reduction

The mean air velocity u , friction factor f , and Reynolds number Re are defined as:

$$u = \dot{V}_a / A_c \quad (1)$$

where \dot{V}_a is the air volume flow rate, and A_c is the cross sectional area of the tested tube.

$$f = \frac{\Delta P}{L/d} \cdot \frac{2}{\rho_a u^2} \quad (2)$$

$$Re = \frac{\rho u d_i}{\mu} \quad (3)$$

The average wall temperature $\Delta T_{w,avg}$ is defined as:

$$T_{w,avg} = \frac{\sum_{i=1}^n T_{wi}}{n} \quad (4)$$

Where n is the number of thermocouples fixed on the inside wall of the test section.

The rate of heat generated through the electric resistance is equal to the heat transfer to the flowing air stream and is calculated by:

$$Q = IV \cos \phi \quad (5)$$

Where $\cos \phi$ is the power factor and is equal to unity.

The average heat transfer coefficient for the inside tube wall is given by:

$$\bar{h} = \frac{\dot{Q}}{A_s (T_{w,avg} - T_b)} \quad (6)$$

Where:

T_b is the bulk air temperature, $(T_i + T_o)/2$, and A_s is the inside surface area of the tube.

The average Nusselt number is calculated by the relation:

$$\bar{Nu} = \frac{\bar{h} d_i}{k_a} \quad (7)$$

4. Results and Discussion

4.1 Plain tube

The results obtained in this study are presented and discussed in this section. Figure (4) and figure (5) show the variation of Nusselt number and friction factor with Reynolds number in case of plain tube. By referring to these figures, as expected, as the Reynolds number increases, Nusselt number increases too; whereas the friction factor decreases and has the same trend as that obtained by Promvonge and Smith, [8]. The present data is matched with the literature value for plain tube with a discrepancy of less than $\pm 9\%$ for Nusselt number and 11% for friction factor.

4.2 Temperature distribution

The variation of local temperature along the tested tube at different turbulator position ratio (X_i/L) and Reynolds number are presented and compared with that of smooth tube are shown in Figs.(6-9). When the turbulator element is placed at inlet to the tested tube, the temperature increases with local distance along the tube. The temperature just after the turbulator element inserts is decreased than that of smooth tube because of the induced turbulence and superimposed vortex motion causing a thinner boundary layer and consequently decreases the wall temperature. Therefore, this vortex begins to decay and the wall temperature begin to increase downwards.

Figure (10) shows the variation of the average wall temperature of the tested tube with turbulator position ratio at constant heat flux and different turbulator element ratios. As expected, the average wall temperature of the tube decreases with increasing Reynolds number because the heat transfer rate depends on the cooling capacity rate of air. It is obvious that at $X_i/L=0.25$, the

average wall temperature of the tube has the lowest values.

4.3 Heat transfer coefficient

The variation of average Nusselt number with Reynolds number for tube fitted with twisted vane turbulator element inserts is shown in figures (11). The figure shows that the average Nusselt number increases with increasing Reynolds number. It also shows that the average Nusselt number for a given Reynolds number is increased with the increase of turbulator element position ratio and attains its maximum value at turbulator position ratio $X_i/L=0.25$. This increase is due to enhanced swirl flow which tends to decrease the boundary layer thickness of the hot air flow and increase residence time of hot air flowing in the tube.

4.4 Friction factor

The pressure drop due to the presence of twisted vane turbulator is the same as its positions are changed. The friction factor in this case is calculated by equation (2) and plotted against Reynolds number as shown in figure (12). As expected, the friction factor decreases with increasing Reynolds number

4.5 Correlation of the present data

The present experimental data are correlated to express friction factor as a function of Reynolds number and Nusselt number as a function of Reynolds number and turbulator position ratio as shown in figures (13). By the mathematical statistical analysis (Least Squares method), a correlation for both friction factor and mean Nusselt number are correlated as:

$$f = 2.5589 \text{ Re}^{-0.4963} \dots\dots\dots (8)$$

$$\bar{Nu} = 0.98932 \text{ Re}^{0.4768} e^{S/L^{-0.0784}} \dots\dots (9)$$

The equations (8, 9) are valid in the ranges $2747 < \text{Re} < 6390$ and $q = 625 \text{ W/m}^2$. The deviation of present experimental results from these correlations are $\pm 10\%$ for Nusselt number and $\pm 5\%$ for the friction factor as shown in figures (14-15).

4.6 Performance evaluation

Webb and Eckert [1], proposed a method of heat transfer efficiency index which takes into account both heat transfer and friction factor as:

$$\eta = \frac{Nu / Nu_s}{(f / f_s)^{1/3}} \quad (10)$$

Throughout the results of the present experimental study, it appears that swirl element led to a higher enhancement in efficiency as can be seen in Fig.(16). It can be seen that the enhancement efficiency decreases as X_i/L decrease which generally higher at high Reynolds number and the maximum enhancement efficiency is found to be 270% associated with Reynolds number of 6390 when the turbulator element at a position of 0.25.

5. Conclusion

The heat transfer augmentation in a circular tube fitted with a twisted vane turbulator inserts at different position has been studied experimentally. In addition, the effect of the turbulator element position on the heat transfer enhancement efficiency is also investigated. It can be concluded that:

1. The secondary fluid motion which is generated by the twisted radial vane turbulator element inserts is resulting twist mixing, and enhance the heat transfer characteristics.
2. The maximum enhancement in heat transfer is 270% ($q = 625 \text{ W/m}^2\text{.K}$, $Re = 6390$, $X_i/L = 0.25$), meanwhile the friction loss increases by about 200%.
3. The obtained correlations of both friction factor and mean Nusselt number in case of twisted radial guide vane turbulator are a helpful tool in this type of heat transfer enhancement mechanisms.

6. Nomenclature

A_c Tube cross-sectional area, m^2
 A_s Surface area of tube, m^2

d_i Inside tube diameter, m
 f Friction factor, -
 h Heat transfer coeff., $\text{W/m}^2\text{.K}$
 I Electric current intensity, A
 k Air thermal conductivity, W/m.K
 L Test section length, m
 m Air mass flow rate, kg/s
 P Pressure, Pa
 p Pitch, m
 q Heat flux, W/m^2
 Q Rate of heat flow, kW
 S Local turbulator position from inlet, m
 s Free spacing, m
 T Temperature, $^\circ\text{C}$
 u Average air velocity inside tube, m/s
 V Air volume flow rate, m^3/s
 X_i Local position from inlet, m

Dimensionless Groups:

Pr Prandtl number
 Re Reynolds number
 Nu Nusselt number

Greek Symbols:

ρ Density, kg/m^3
 μ Dynamic viscosity, kg/m.s
 $\cos \phi$ Power factor, -
 η Heat transfer efficiency index, -

Sub-Scripts:

a Air
 b Bulk
 i Inlet
 o Outlet
 Avg Average
 s Surface

7. References

- [1] Webb, R.L., Eckert, E.R.G., "Application of rough surfaces to heat exchanger design". *Int. J. Heat Mass Transfer*, 15, 1647-1658, 1972.
- [2] Hong, S. W., Bergles, A. E., "Augmentation of laminar heat transfer in tubes by means of twisted tapes inserts". *J. Heat Transfer*, 98, pp.252-256, 1976.

- [3] Manglik, R. M., Bergles, A. E., " Heat transfer and pressure drop correlations for twisted tape inserts isothermal tubes: (I) Laminar flows". J. Heat Transfer, 115, pp.881-889, 1993.
- [4] [2] Manglik, R. M., Bergles, A. E., " Heat transfer and pressure drop correlations for twisted tape inserts isothermal tubes: (II) Transition and turbulent flows". J. Heat Transfer, 115, pp.890-896, 1993.
- [5] Sarma, P. K., Subramanyam, T., Kishore, P. S., Dharma Rao, V., Sadik Kakac, "Laminar convective heat transfer with twisted tape insets in a tube". Int. J. Thermal Science, 42, pp.821-828, 2003.
- [6] Neshumayev, D., Ots, A., Laid, J., Tiikma, T., "Experimental investigation of various turbulator inserts in gas heated channels". Experimental Thermal Fluid Science, 28, pp.877-886, 2004.
- [7] Leonard D. Tijing, Bock Choon Pak, Byung Joon Beak, Dong Hwan Lee, " A study on heat transfer enhancement using straight and twisted internal fin inserts". Int. Communication in Heat and Mass Transfer, Vol.(33), pp. 719-726, 2006.
- [8] Smith Eiamsa-ard, Pongjet Promvonge, " Experimental investigation of heat transfer and friction characteristics in circular tube fitted with V-nozzle turbulators". Int. Commun. Heat Mass Transfer, 33(5), 591-600, 2006.
- [9] Watcharin Noothong, Smith Eiamsa-ard, and Pongjet Promvonge, " Effect of twisted tape inserts on heat transfer in a tube". 2nd Int. Conference on Sustainable Energy and Environment (DEE 2006), 21-23 November 2006, Bangkok, Thailand, pp.1-5.
- [10] Promvonge P., and Eiamsa-ard S., " Heat transfer behaviors in a tube with combined conical ring and twisted tape inserts". Int. Communication in Heat and Mass Transfer, Vol.(34), pp. 849-859, 2007.
- [11] Paisarn Naphon, " Laminar convective heat transfer and pressure drop in the corrugated channels". Int. Communication in Heat and Mass Transfer, Vol.(34), pp. 62-71, 2007.
- [12] Mehmet Yilmaz, Omer Comakli, Sinan Yapici, and O. Nuri Sara, " Heat transfer and friction characteristics in decaying swirl flow generated by different radial guide vane swirl generators". Energy Conservation & Management, 44 (2003), 283-300.
- [13] Smith Eiamsa-ard, Chinaruk Thianpong and Pongjet Promvonge, " Experimental investigation of heat transfer and pressure drop characteristics of flow through circular tube filled with regularly spaced twisted tape". Int. Conference on Sustainable Energy and Environment (SEE), 1-3 December 2004, Hua Hin, Thailand, 18-22.
- [14] Ebru Kavak Akpınar, Yasar Bicer, Cengiz Yildiz, Dursun Pehlivan, " Heat transfer enhancement in a concentric double pipe exchanger equipped with swirl element". Int. Comm. Heat Mass Transfer, Vol.32, No.6, pp.857-868, 2004.
- [15] Hong Mengna, Deng Xianhe, Huang Kuo, and Li Zhiwu, "Compound heat transfer enhancement of a converging-diverging tube with evenly spaced twisted-tapes". Chin J. Chem. Eng., 15(6), 814-820, 2007.
- [16] Smith Eiamsa-ard, Somsak Pethkool, Chinaruk Thianpong and Pongjet Promvonge, " Turbulent flow heat transfer and pressure loss in a double pipe heat exchanger with louvered strip inserts". Int. J. Heat Mass Transfer, 35, 120-129, 2008.

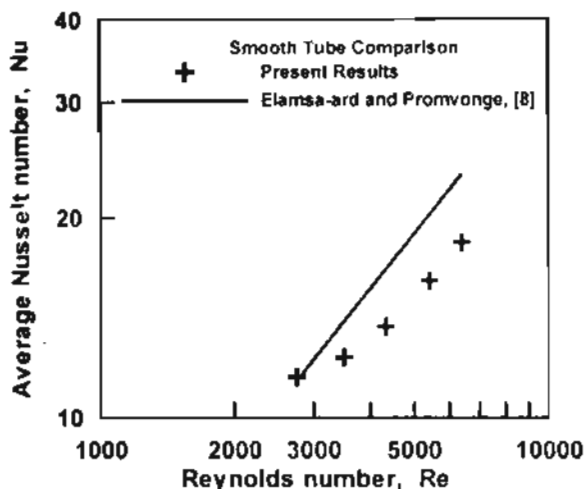


Figure (4) Comparison of the present experimental results with the published data, [8].

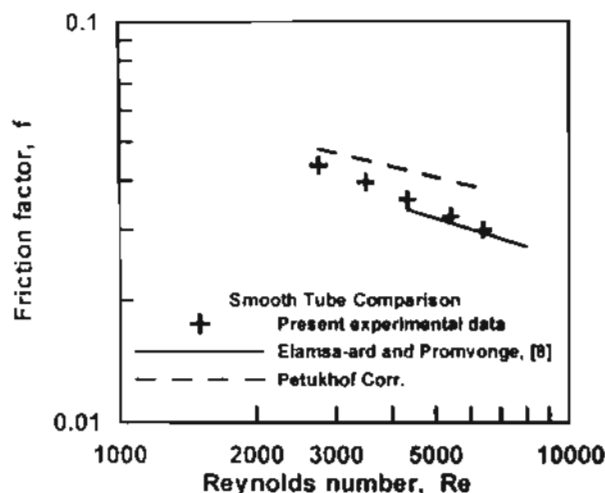


Figure (5) Comparison of the present experimental results with the published data.

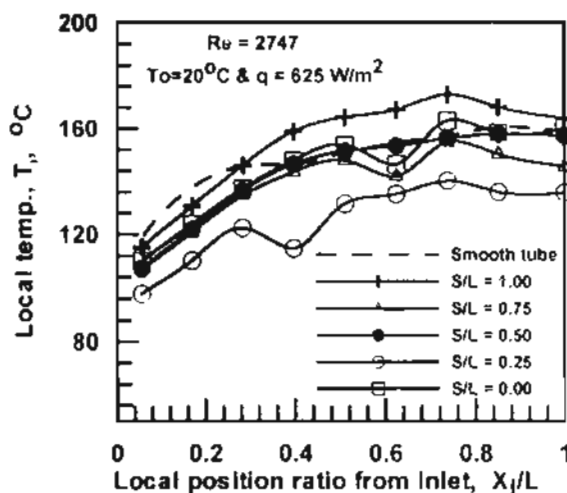


Figure (6) Local wall temperature distribution with dimensionless distance from inlet at constant Reynolds number and different turbulator position.

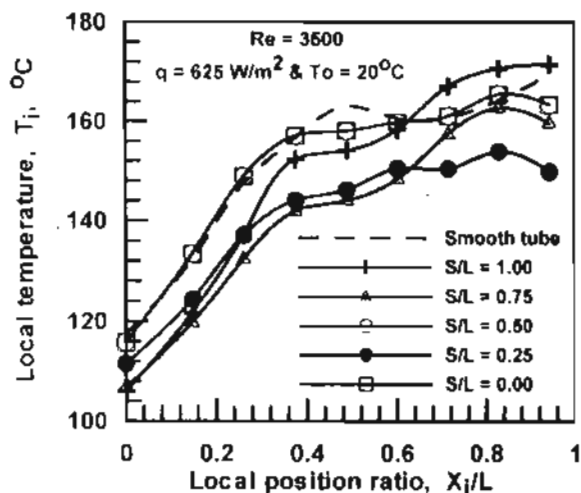


Figure (7) Local wall temperature distribution with dimensionless distance from inlet at constant Reynolds number and different turbulator position.

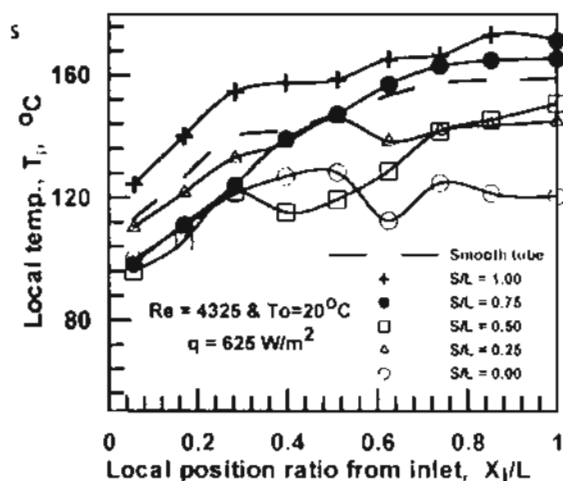


Figure (8) Local wall temperature distribution with dimensionless distance from inlet at constant Reynolds number and different turbulator position.

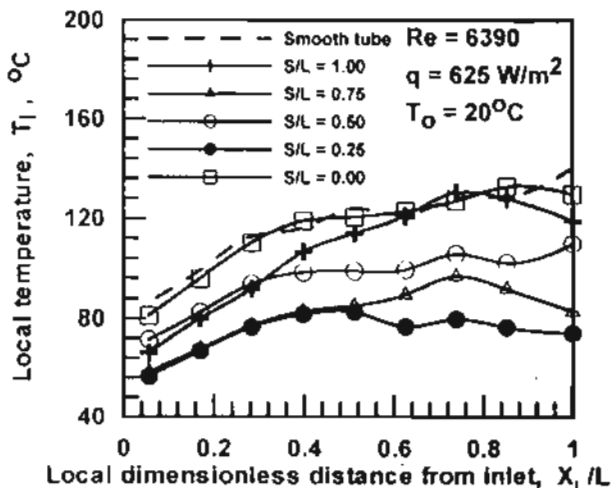


Figure (9) Local wall temperature distribution versus dimensionless distance at constant Reynolds number and different turbulator position.

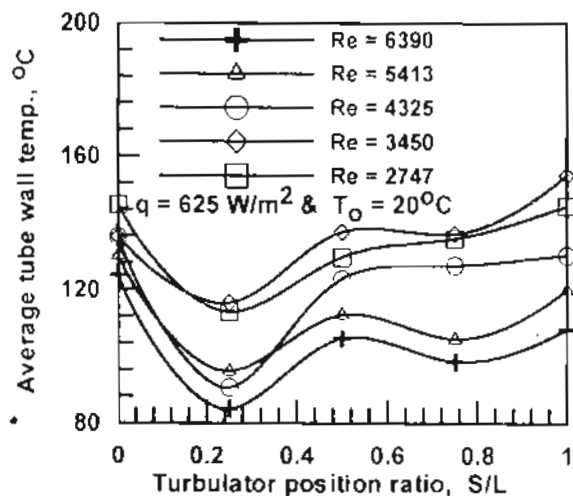


Figure (10) Average tube wall temperature versus the turbulator element position at constant heat flux and different Reynolds number.

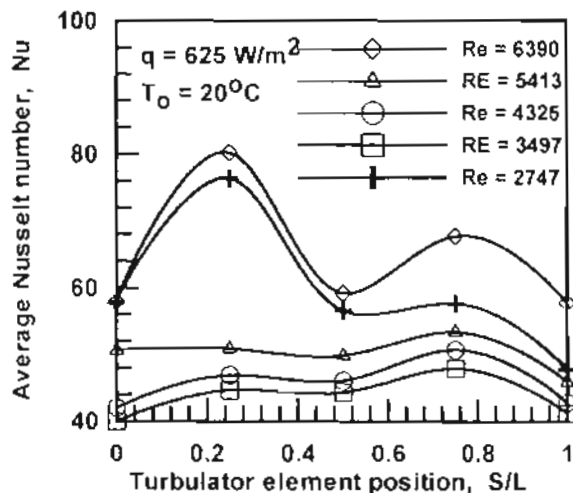


Figure (11) Average Nusselt number versus turbulator position ratio from inlet to the test section at constant both Reynolds number and heat flux.

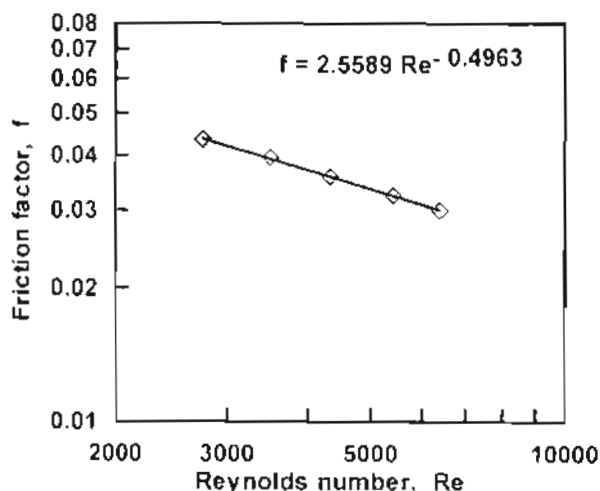


Figure (12) Friction factor versus Reynolds number for the present data in the presence of twisted vane turbulator inserts.

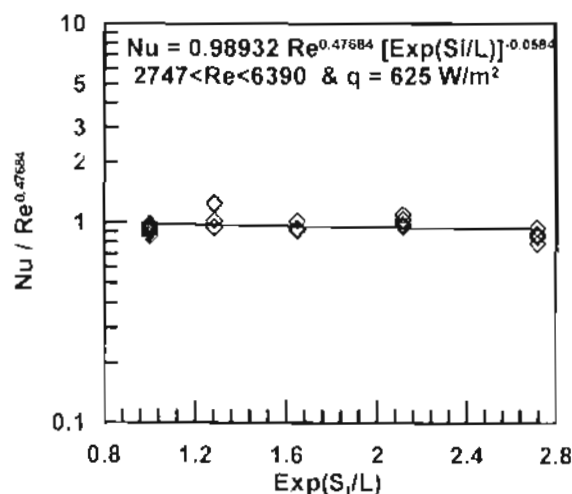


Figure (13) Correlation of present experimental results

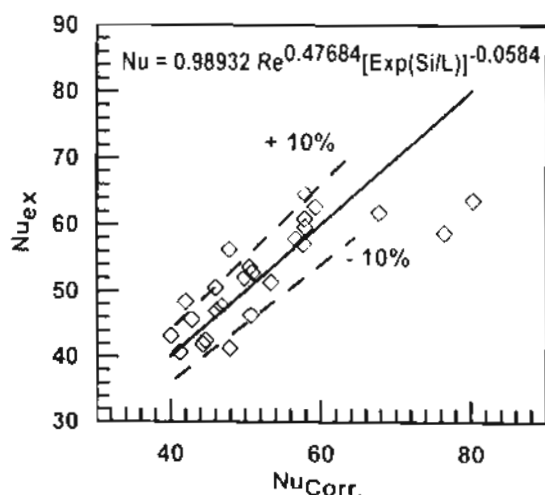


Figure (14) Deviation of present experimental results from the present correlation

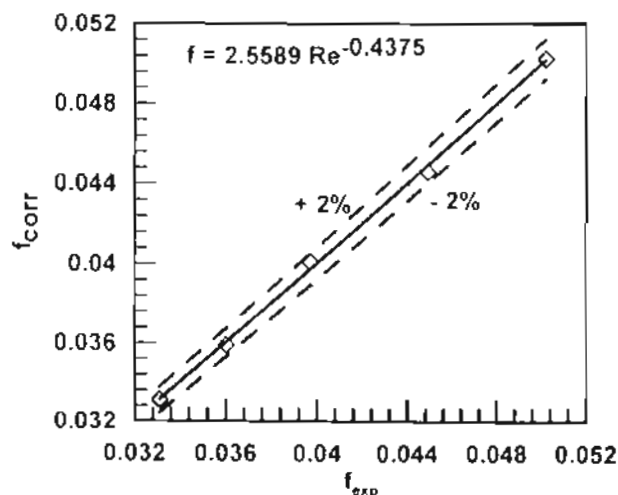
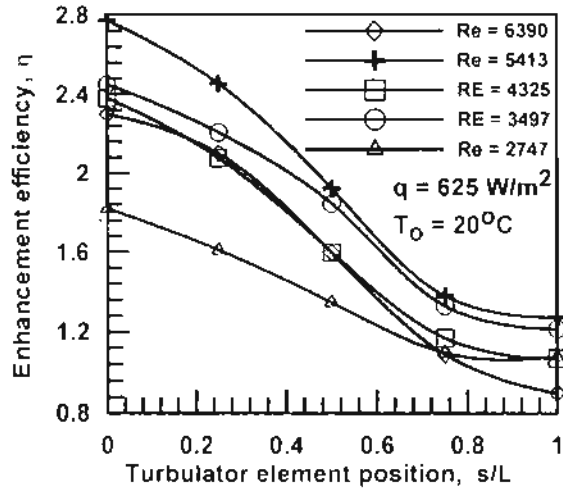


Figure (15) Deviation of the present experimental data of friction factor from that of the correlated value



Figure(16) Performance evaluation of tube fitted with turbulator element for different Reynolds number and constant heat flux